An Experimental Study of Slip Flow in Capillaries and Semihyperbolically Converging Dies

P.A. Kamerkar, B.J. Edwards
Department of Chemical Engineering, University of Tennessee, Knoxville, TN 37996

Slip velocity is measured in straight-walled capillary dies and semihyperbolically converging dies (SHCDs) in three industrial polymer melts, with and without the presence of a viscosity reducing stearic acid (SA) additive. Data taken in shear flow through capillary dies indicated a substantial increase in the slip velocity caused by the addition of the SA. Data taken in the SHCDs showed much less of an increase in the slip velocity of the polymer/additive system relevant to the neat polymer. One possible explanation of this observation is that the magnitude of the slip velocity is directly related to the degree of orientation within the flowing polymeric material. POLYM. ENG. SCI., 47:159–167, 2007. © 2007 Society of Plastics Engineers

INTRODUCTION

In fluid flow through a capillary, the "no-slip" boundary condition at the walls is usually assumed. This condition implies complete adhesion of the fluid to solid boundaries. However, this assumption does not always hold true. Many times, it has been observed that the fluid slips at the wall, and has a nonvanishing velocity at the solid interface. This often results in extrudate abnormalities, such as sharkskin, stick-slip melt fracture, etc. [1–11]. It has been observed that, in capillary flows, the no-slip condition typically does not hold beyond a critical value of shear stress [3].

Many researchers have tried to study the nature of slip and the causes behind it. From the findings of Kalika and Denn [3], in the study of capillary extrusion of linear low-density polyethylene (LDPE), one can get a good idea of transitions that occur between various flow regimes. They report a stable flow region below a critical value of the shear stress, where a smooth and regular extrudate is produced. At the critical stress, they observed the onset of the sharkskin texture, after which the extrudate showed high-frequency surface variations. At higher stresses, the extrudate showed alternating regions of smooth surface and sharkskin. At even higher stresses, melt fracture was observed, which was indicated by a grossly distorted extrudate. In all, there seems to be a general agreement among researchers that the main cause of slip and the resulting onset of surface irregularities in the extrudate is the breakdown of the adhesion between the polymer and metal interface [1, 3, 5, 6].

During extrusion, the extrudate abnormalities are first observed when the volumetric flow rate exceeds a critical value. As the flow rate increases, the amplitude of these distortions also increases. These instabilities in the flow give rise to extrudate surface defects, and hence the production rates of commercially available products are limited to flow rates below the critical values. This is economically taxing, and hence to improve the process, aids are frequently used.

Processing aids help eliminate these flow instabilities, or at least help delay their occurrence to higher flow rates. Processing aids used typically include various types of additives or surface coatings. When used in low concentrations, dispersed in the neat polymer, additives act as lubricants. They reduce the apparent viscosities, and hence the reduced values of pressures can be used in extrusion. Surface coatings modify the melt-wall interactions and decrease the shear stress required for a specific flow rate. They also prevent the rupture of the polymer as it exits the die. Fluoropolymers, stearates, hydrocarbons, boron nitride, and carboxylic acids are examples of some additives that have been the subject of active research in past years [12–24].

It is quite reasonable to speculate that the degree of adhesion and stick at the walls in capillary flows is somehow related to the degree of orientation induced in the fluid as the material flows through the device. The higher the shear rate, in principle, the higher the degree of orientation of the chain molecules comprising the fluid. As the molecules stretch out and orient in response to the forces imparted by the flow field, their adhesive characteristics can be altered dramatically, leading to the high strain-rate anomalies mentioned earlier. Although this orientation

Correspondence to: B.J. Edwards; e-mail: bjedwards@chem.engr.utk.edu
Current address for P.A. Kamerkar is Anton PAAR USA, Ashland, VA 23005
Contract grant sponsor: Department of Chemical Engineering, University of Tennessee.
DOI 10.1002/pen.20692
Published online in Wiley InterScience (www.interscience.wiley.com).

effect seems very plausible, we know of no other experimental studies that set out explicitly to investigate it.

In this article, we examine the effects of orientation on the adhesive characteristics of several typical industrial polymer melts through a comparison of experimental data taken in both straight-walled capillary tubes and semihyperbolically converging dies (SHCDs). This is accomplished by comparing stress data for each neat polymer from both geometries with similar data taken for each polymer with a viscosity-reducing additive. As discussed below, for a given applied pressure drop, the degree of orientation induced in the SHCDs is much greater than that in the capillary dies. Hence, the degree of reduction in the stress versus strain-rate curves can provide indications of the degree of adhesion of the neat polymer as a function of orientation, as discussed below.

In the following section, we provide a brief overview of the use of capillaries and SHCDs for determining viscosities and slip velocities of polymeric materials. Although this material is standard for capillary dies, for the SHCDs, we have to develop some new approximate equations to relate pressure drop to slip velocity. In Experimental Section, we present the details of the experimental measurements, i.e., equipment, materials, etc. In Results and Discussion Section, we present our experimental results and discuss their implications in depth. Summary offers our conclusions from this research.

VISCOSITIES AND SLIP VELOCITIES IN CAPILLARIES AND SEMIHYPERBOLICALLY CONVERGING DIES

Mooney's Analysis for Capillary Flow

In 1931, Mooney [25] derived a methodology for quantifying the slip velocity in straight-walled capillary tubes. Although this analysis is standard and well-known, we present it here in some detail since we will alter it in the next subsection for the SHCDs; it is therefore instructive to consider first the details of the simpler analysis for capillaries.

In capillary rheometry, the Hagen-Poiseuille law quantifies the relationship between the fluid flow rate through the tube, and the pressure drop over the tube length. This expression is

$$Q = \frac{\pi \Delta P R^4}{8\eta L}, \tag{1}$$

where Q is the volumetric flow rate, $\Delta P = P_0 - P_L$ is the pressure drop between the inlet (P_0) and outlet (P_L) pressures, R is the tube radius, L is the tube length, and η is the shear viscosity of the fluid. Note that this expression only applies to a fluid with a constant viscosity (i.e., a Newtonian fluid), and was derived under the no-slip boundary condition. In a typical experiment of a Newtonian fluid, the flow rate is measured as a function of the applied pressure drop, allowing calculation of the shear viscosity from *Eq. 1* as a function of pressure drop.

In the case of a non-Newtonian fluid, the procedure for calculating the viscosity from the flow rate versus ΔP data is more complicated. The shear stress at the capillary wall, $\sigma_{rz}(R) \equiv \sigma_w$ (for flow in the z direction with r as the radial direction), is given by

$$\sigma_w = \frac{\Delta P R}{2L}, \tag{2}$$

and the Weissenberg-Rabinowitsch equation allows calculation of the wall shear rate,

$$\dot{\gamma}_w = \frac{1}{\sigma_w^2}\frac{d}{d\sigma_w}\left(\sigma_w^3 \ \frac{Q}{\pi R^3}\right), \tag{3}$$

with Q given by *Eq. 10*, below. The shear viscosity at the wall is then calculated using the equation

$$\eta(R) = -\frac{\sigma_w}{\dot{\gamma}_w}. \tag{4}$$

All of the above-mentioned standard equations of capillary viscometry were developed using the no-slip velocity condition, discussed in the introductory section of this article. Mooney generalized these equations to allow for the calculation of a nonvanishing fluid velocity at the fluid/wall interface, i.e., the "slip velocity." The shear stress at any radial location within the capillary is given by

$$\sigma_{rz}(r) = \frac{\Delta P r}{2L}. \tag{5}$$

For $r = R$, *Eq. 2* ensues. Since the velocity in the z direction, v_z, is assumed to be a function of r only, it may be calculated at any point within the tube through the equation

$$\int_{v_z(R)}^{v_z(r)} dv_z = \int_R^r \frac{dv_z(r')}{dr'} dr'. \tag{6}$$

The stress at any point in the tube is defined as

$$\sigma_{rz}(r) \equiv -\eta(r)\frac{dv_z(r)}{dr}, \tag{7}$$

so that *Eq. 6* can be written as

$$v_z(r) = v_z(R) + \int_r^R \frac{\sigma_{rz}(r')}{\eta(r')} dr' \equiv v_{slip} + \int_r^R \frac{\sigma_{rz}(r')}{\eta(r')} dr'. \tag{8}$$

Consequently, the velocity at any point can be written using *Eqs. 2* and *5* as

$$v_z(r) = \frac{R\Delta P \beta}{2L} + \int_r^R \frac{r'\Delta P}{2L\eta(r')} dr', \tag{9}$$

 DOI 10.1002/pen

where β is called the coefficient of slip at the wall shear stress, σ_w, defined through the relationship $v_{slip} \equiv \sigma_w \beta$.

The rate of flow through the capillary can be calculated from $Q = \int_0^R 2\pi r v_z(r) dr$ using *Eq. 9*. It can thus be determined through integration by parts as the expression

$$Q = \frac{\pi \Delta P R^3 \beta}{2L} + \frac{\pi \Delta P}{2L} \int_0^R \frac{r^3}{\eta(r)} dr. \tag{10}$$

Note that when $\beta = 0$ and η is constant, *Eq. 10* reduces to the Hagen-Poiseuille law, *Eq. 1*. By inverting *Eq. 5*, the independent variable in this equation can be switched from r to σ_{rz}. Thus, in view of *Eq. 2*, *Eq. 10* becomes

$$Q = \pi R^2 \sigma_w \beta + \frac{\pi R^3}{\sigma_w^3} \int_0^{\sigma_w} \frac{\sigma_{rz}^3}{\eta(\sigma_{rz})} d\sigma_{rz}. \tag{11}$$

Dividing this expression by πR^3, and then taking the derivative with respect to $\frac{1}{R}$ holding σ_w fixed, yields the "Mooney equation,"

$$\left. \frac{\partial \left(\frac{Q}{\pi R^3} \right)}{\partial \left(\frac{1}{R} \right)} \right|_{\sigma_w} = \sigma_w \beta = v_{slip}. \tag{12}$$

With this expression, the slip velocity can be determined as a function of wall shear stress by making measurements of the same test fluid in capillaries of varying radius.

Analysis of the Slip Velocity in Semihyperbolically Converging Dies

The semihyperbolically converging die is a tube with a radius that changes as a function of axial distance [26, 27]:

$$R(z) = \sqrt{\frac{C}{z + B}}, \tag{13}$$

where the constants B and C are determined by

$$B = L \frac{R_e^2}{R_0^2 - R_e^2} \qquad C = L \frac{R_0^2 R_e^2}{R_0^2 - R_e^2}, \tag{14}$$

in terms of the entrance, $R(0) = R_0$, and exit, $R(L) = R_e$, radii of the die. According to *Eq. 13*, the radius of the tube is much greater at the entrance to the die than at the exit, and there is a hyperbolic relationship of radius between the entrance and exit of the die. R_0 and R_e can be chosen such that dies with integer values of the Hencky strain, ε_h, can be manufactured [26, 27]; in our experiments, we used SHCDs possessing Hencky values of 4, 5, 6, and 7. In terms of the design parameters, the Hencky value of a specific die is determined by the relationship $\varepsilon_h = \ln\left(R_0^2 / R_e^2 \right)$ [28].

In the SHCD, the flow field is much more complicated than for the straight-walled capillary tube. In this case, not only are shear effects present, but the primary kinematics within the die are those of uniaxial elongational flow. Thus, there is typically a mixture of both types of flow within the die. In the case of full-slip conditions (no adhesion between the fluid and the die wall), Feigl et al. [28] showed that the kinematics within the die were virtually indistinguishable from those of purely uniaxial elongational flow. However, for no-slip conditions, there is a substantial boundary layer near to the wall in which shear effects play a dominant role in the local fluid kinematics [28]. This boundary layer is rather thin in general, and decreases in magnitude and thickness for varying degrees of slip at the wall. In the SHCD, the average strain rate (see below for the definition of this quantity) is much lower than in the capillary die; however, the degree of orientation induced within the test fluid is much greater because of the substantial contribution of the elongational kinematics.

Unless the longest relaxation time of the test fluid is less than the residence time of a fluid element with the SHCD, the fluid will not achieve steady state in a Lagrangian sense, although the pressure drop measured for a given flow rate will achieve a steady-state value. Consequently, a true elongational viscosity of the test fluid cannot be obtained in this fashion; however, an "effective elongational viscosity," η_e, can be determined. This effective viscosity is defined as [26, 27]

$$\eta_e = \frac{\Delta P}{\dot{\varepsilon}\, \varepsilon_h}, \tag{15}$$

where $\dot{\varepsilon}$ is the effective strain rate in the SHCD, expressed by [28]

$$\dot{\varepsilon} = \frac{Q}{\pi R_0^2 L} (\exp(\varepsilon_h) - 1). \tag{16}$$

According to Ref. 28, when the fluid experiences full-slip conditions at the wall, all streamlines have this value of strain rate, which is independent of axial position. For no-slip conditions, and those in between these two extremes, *Eq. 16* still quantifies the average strain rate within the die [28].

Now, we wish to extend the Mooney analysis for capillary tubes to the SHCDs; however, this becomes much more difficult because of the strong presence of extensional characteristics in the flow kinematics. For no-slip boundary conditions, the shear effects in these dies are small and limited to a boundary region near the wall [28]. As the degree of slip increases, the shear region is confined closer to the wall, until it eventually disappears completely for full-slip boundary conditions. Performing a similar derivation to the Mooney analysis for capillaries is very difficult for the SHCD under general conditions. This would involve numerical integration of the partial differential equations for the momentum equation, coupled

with a constitutive model for the fluid under investigation. Although such a detailed simulation might be warranted for future work, in the meantime, we need some approximate method by which we can judge whether or not our gross hypothesis is correct. In other words, we want to make some limiting assumptions, whereby we can derive an approximate version of the Mooney equation to judge if the SHCD does really indicate a direct relationship between degree of induced orientation and slip at the die wall.

The assumption that we are going to make to simplify the analysis is as follows. We are going to assume a priori that a fair degree of slip is occurring within the SHCD. According to the results of Feigl et al. [28], the shear effects are then all contained within a very thin boundary layer near the die wall. As such, the bulk of the fluid within the die is experiencing purely uniaxial elongational flow. Hence, the pressure drop measured by the die is almost entirely because of the elongational kinematics. Whether or not this assumption is valid can be indirectly tested experimentally by comparing measured pressure drops in the dies for neat polymers with those for the same polymers mixed with viscosity reducing additives. These experiments have been carried out, as described below, and seem to indicate that this assumption is reasonably valid.

On the basis of our assumption, the bulk fluid within the SHCD will follow the stream function, Ψ, imposed by the shape of the die. Therefore, we can set [28]

$$\Psi = -\frac{r^2 z}{2}, \tag{17}$$

which implies that

$$d\Psi = -rz\ dr - \frac{r^2}{2} dz. \tag{18}$$

Along any particular streamline, $d\Psi = 0$, so that $dr = -\frac{r}{2z} dz$.

In the SHCD, the z-component of the velocity field is a function of both r and z. Consequently, in view of *Eq. 18* and the definitions $\dot{\gamma} = \frac{\partial v_z}{\partial r}$ and $\dot{\varepsilon} = \frac{\partial v_z}{\partial z}$, the differential of the velocity component in the z-direction is

$$dv_z = \dot{\gamma}\ dr - \frac{2\dot{\varepsilon} z}{r} dr. \tag{19}$$

Note that the shear stress is still defined by $\sigma_{rz}(r,z) = -\eta(r,z)\dot{\gamma}(r,z)$, and that $\dot{\varepsilon}$ is a constant under our original assumption. Therefore, at any location within the die, v_z is given by the integral expression

$$v_z(r,z) = v_{\text{slip}}(z) + \int_r^R \frac{\sigma_{rz}(r',z)}{\eta(r',z)} dr' - 2\dot{\varepsilon} z\ \ln\frac{r}{R}. \tag{20}$$

This equation should be valid near to the wall of the die under our primary assumption. As before, v_{slip} can be expressed as $v_{\text{slip}} = \sigma_w\ (z)\ \beta$, where σ_w is the shear stress at the wall.

Since the radius of the die changes axially, the volumetric flow rate divided by πR^3 $\left(\hat{Q} = \frac{Q}{\pi R^3}\right)$ in the die is also a function of z. The expression for the flow rate is given by

$$\hat{Q}(z) = \frac{1}{\pi R^3} \int_0^R 2\pi r v_z(r,z) dr, \tag{21}$$

so that the substitution of *Eq. 20* into this expression yields

$$\hat{Q}(z) = \frac{1}{\pi R^3} \left[\pi R^2 \sigma_w(z)\beta + 2\pi \int_0^R r \left(\int_r^R \frac{\sigma_{rz}(r',z)}{\eta(r',z)} dr' \right) dr - 4\pi\dot{\varepsilon} z \int_0^R r \ln\frac{r}{R} dr \right]. \tag{22}$$

Performing the integrations over r in this expression, we obtain

$$\hat{Q}(z) = \frac{1}{\pi R^3} \left[\pi R^2 \sigma_w(z)\beta + \pi \int_0^R r^2 \frac{\sigma_{rz}(r,z)}{\eta(r,z)} dr + \pi\dot{\varepsilon} z R^2 \right]. \tag{23}$$

In the shear layer near the wall, the shear stress is still proportional to r, as in the Mooney analysis, so that changing variables from r to σ_{rz} yields

$$\hat{Q}(z) = \frac{1}{\pi R^3} \left[\pi R^2 \sigma_w \beta + \frac{\pi R^3}{\sigma_w^3} \int_0^{\sigma_w} \frac{\sigma_{rz}}{\eta(\sigma_{rz},z)} d\sigma_{rz} + \pi\dot{\varepsilon} z R^2 \right]. \tag{24}$$

Finally, moving the last term on the right side over to the left side, and differentiating with respect to $\frac{1}{R}$, gives

$$\left. \frac{\partial \left(\frac{Q}{\pi R^3} - \frac{\dot{\varepsilon} z}{R} \right)}{\partial \left(\frac{1}{R} \right)} \right|_{z,\sigma_w} = \sigma_w \beta = v_{\text{slip}}. \tag{25}$$

Equation 25 is the SHCD equivalent of the Mooney equation for a straight-walled capillary; however, it is very important to keep in mind the assumption under which it was derived. The Mooney equation is universally valid, whereas *Eq. 25* is only correct if the assumptions leading to it are valid. Consequently, the fluid within the die has to experience a large degree of slip for the preceding analysis to quantify even approximately the slip velocity of the fluid.

EXPERIMENTAL

We conducted experiments using three typical, industrially important polymers, ASTM D1238 polypropylene (PP), low-density polyethylene (LDPE), and high-density polyethylene (HDPE), both obtained from ExxonMobil.

 DOI 10.1002/pen

The melt indices of these polymers were 2.4, 0.75, and 0.24 g/min, and the densities at ambient conditions were 0.90, 0.915, and 0.964 g/ml.

As an additive to the neat polymers, we used commercially available stearic acid (SA), obtained from Fisher Scientific. The molecular weight of the SA was 284.49 g/mol, and its melting and boiling points at 1 atm. were reported as 68 and 361°C, respectively. This compound was chosen as the additive because it is known to act as a lubricant when combined with typical industrial polymers [12]. In our initial experiments, various weight percentages of SA were added to the neat polymers (1, 2, and 5%). These results are discussed below. After the preliminary analysis was completed, we used 2% mixtures to perform experiments to quantify the degree of slip at the die wall. The SA was added to the neat polymer using a twin-screw extruder at 200°C. The extrudate was then pelletized using an in-line pelletizer. All of the experiments were conducted at 220°C.

Stress measurements were performed using the Advanced Capillary Extrusion Rheometer (ACER) and the Advanced Rheometric Expansion System (ARES), manufactured by Rheometric Scientific®. ACER can be fitted with either the straight-walled capillary tubes or the SHCDs. All dies were manufactured from the same material (stainless steel), and were 25 mm in length. For imposed values of the flow rate, the pressure drop over the length of the die is measured via transducer. ARES, a rotational viscometer, was used with a cone-and-plate geometry. For imposed values of rotation of the plate, a transducer measures the torque applied by the test fluid to the cone. ARES was used to measure the shear viscosities of the samples at low shear rates. ACER was used to measure the shear viscosities at high shear rates, and also the apparent elongational viscosities of the samples using the SHCDs. Steady shear viscosity data were obtained over a broad range of shear rates (0.01–10,000 s^{-1}). Apparent elongational viscosity data was obtained with SHCDs of applied Hencky strain values 4, 5, 6, and 7 over effective elongation rates of roughly 1–1000 s^{-1}.

RESULTS AND DISCUSSION

Determination of Lubricant Concentration for Experimental Measurements

The three polymers examined in this work were characterized using ARES to determine the extent of reduction in the shear stress values due to the additive. Three different weight percentages of SA, 1, 2, and 5%, were tested. Steady shear-rate sweeps were performed on all samples using the cone-and-plate geometry at 220°C.

In Figure 1, shear stress versus shear rate is plotted for neat PP and the polymer including three concentrations of SA. We observed a reduction in the apparent shear stress in all samples that contained SA. For PP +1% SA, the extent of reduction averages about 30% over the whole range of shear rates examined herein. The extent of reduction increases for the 2% sample to an average of 40%, but increasing the additive to 5% seems to have no further effect on viscosity reduction. Presumably, once the lubricant has completely coated the walls of the measuring instrument, no further increase in additive concentration will drastically alter the viscous properties of the neat polymer. (Of course, this explanation is under investigation herein. The action of the additive may be thermodynamic, as opposed to kinetic. If the additive induces greater flexibility in the polymer chain architecture, its action would be to lower viscous effects because of the conformational rearrangements in the neat polymer. Such an effect would probably be mitigated at increased additive concentrations.)

Figure 1 also presents similar data for HDPE, with and without the additive. Again, there seems to be an upper limit of concentration, this time at 1% SA, after which no further viscosity reduction is evident. For 1% SA, the shear stress reduction averaged about 27%, whereas for 2% SA, the average was 28%. The LDPE showed similar results to HDPE. Consequently, in the ensuing experiments, we used only one concentration of SA, 2%, since the maximum viscosity reduction occurred for all three neat polymers at this percentage.

Steady-State Shear Flow in Capillary Dies

Experiments with ACER for the three neat polymers and the polymer plus 2% SA were carried out using six capillary dies with different diameters: 0.9, 1.0, 1.25, 1.5, 1.75, and 2.0 mm. All experiments were conducted at 220°C. Figures 2 and 3 show sample results for the effect of the SA additive on the shear stress of the three polymers at higher shear rates than those obtained using ARES, which were displayed in Figure 1. For all three

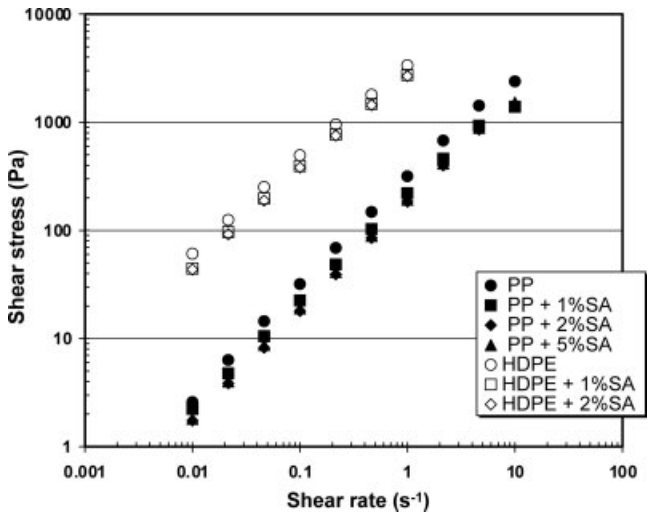

FIG. 1. Effects of the stearic acid additive on the shear stress of PP and HDPE in steady shear flow using a cone-and-plate geometry.

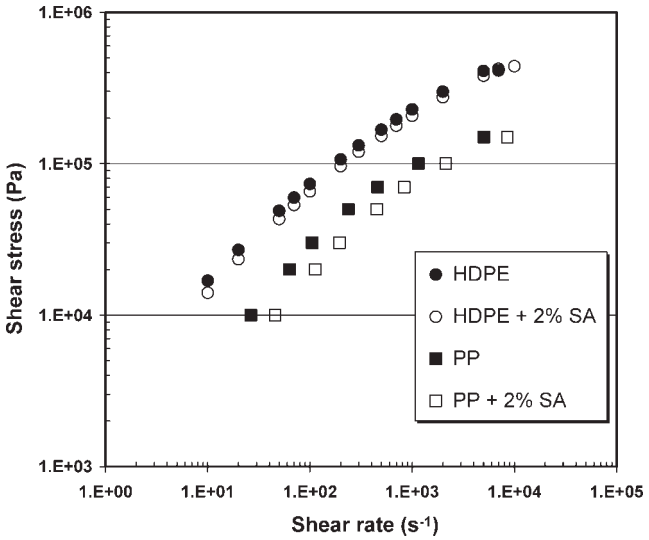

FIG. 2. Shear stress versus apparent shear rate for PP and PP +2% SA in a capillary die of diameter 0.9 mm, and the same for HDPE and HDPE +2% SA in a capillary die of diameter 1.25 mm.

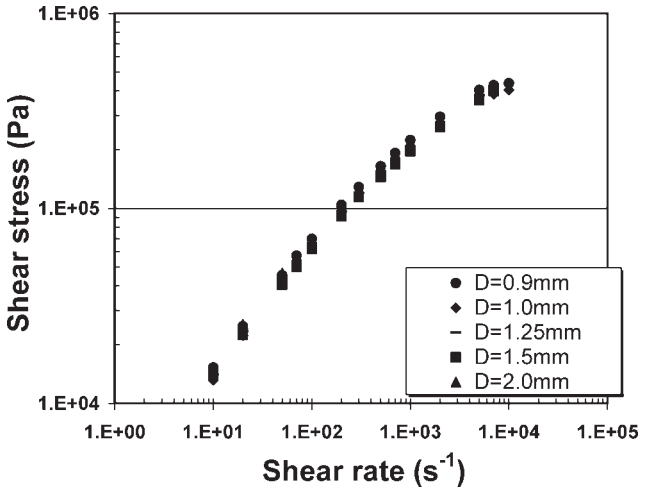

FIG. 4. Shear stress versus apparent shear rate in capillaries of various diameters for HDPE +2% SA.

polymers and for all sizes of die diameter, the degree of stress reduction is largest in the low shear rate regime, ranging from 15–30%, and roughly 5% for very high shear rates where the polymer experiences a high degree of shear thinning. This lends credence to the notion that the viscosity reducing action of the additive is to allow for greater chain flexibility in intramolecular conformational rearrangements of the individual polymer structures. It is well known that the degree of shear thinning is determined by the conformational and orientational state of the flowing polymer chains: at higher shear rates, the chain are more stretched and oriented toward the direction of flow, thereby mitigating to some degree the increased shear force within the fluid. Consequently, as the molecules become more fully extended, the additive effects are also mitigated. Hence the SA has minimal, if any, impact on the measured viscosities at very high shear rates.

Figure 4 displays typical shear stress data as a function of capillary diameter, in this case for HDPE with 2% SA. This data allows us to calculate the slip velocity of the fluid within the dies as a function of wall shear stress, as described earlier. As one would expect, the stresses measured in different dies are much less spread out for the HDPE +2% SA melt than with the neat polymer (not shown), since the slip velocity is greater for the samples with the additive.

To perform the Mooney analysis, we need to use the data from the measurements of the sort displayed in Figure 5 at specified values of the wall shear stress. Hence, the data from the six capillary dies of varying diameter are collected at wall shear stress values of 0.01, 0.02, 0.03, 0.05, 0.07, 0.1, and 0.15 MPa. Thus plots of $\frac{Q}{\pi R^3}$ vs.

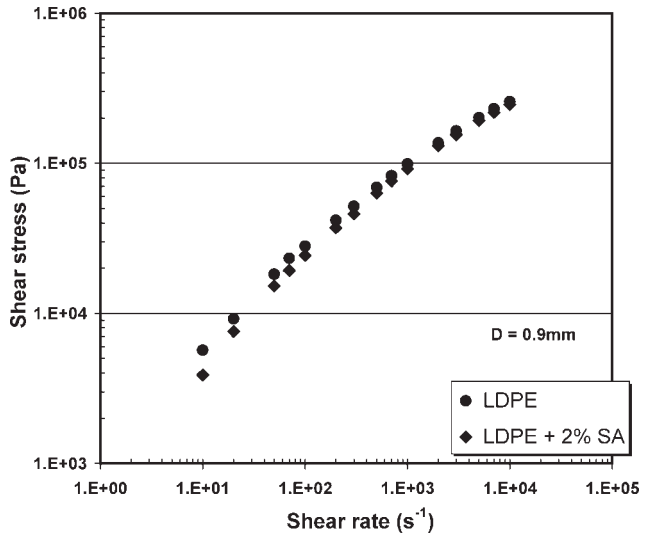

FIG. 3. Shear stress versus apparent shear rate for LDPE and LDPE +2% SA in a capillary die of diameter 0.9 mm.

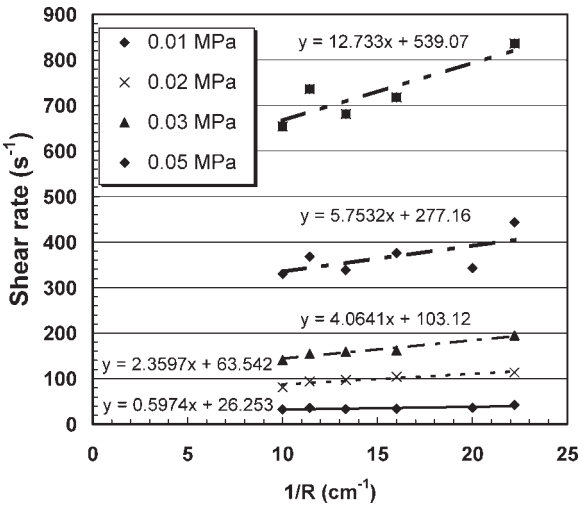

FIG. 5. Plot of apparent shear rate versus reciprocal radius of capillary die at various constant values of the wall shear stress for PP +2% SA.

DOI 10.1002/pen

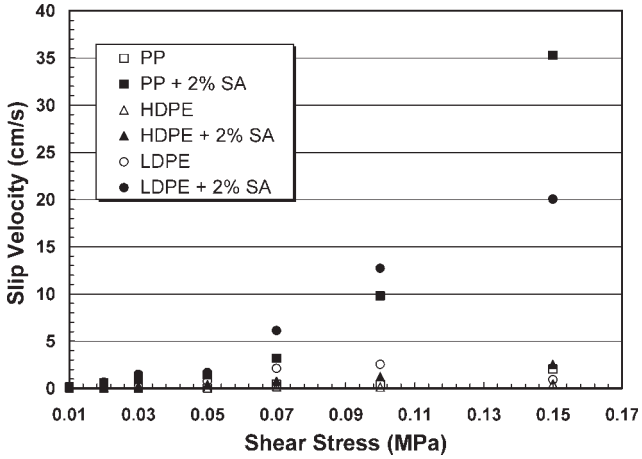

FIG. 6. Slip velocity versus shear stress for all three polymers, with and without additive.

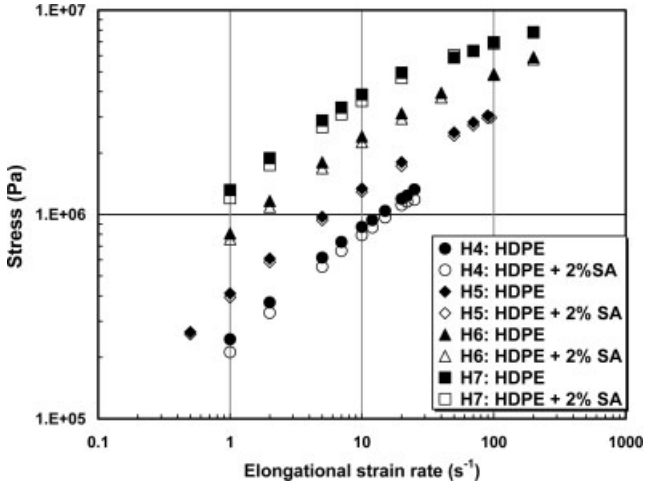

FIG. 7. Effective elongational stress versus strain rate for HDPE and HDPE +2% SA in SHCDs of Hencky values 4, 5, 6, and 7.

$\frac{1}{R}$ at constant wall stress values will yield the slip velocities that we seek. In the sample plot for PP +2% SA of Figure 5, the apparent shear rate, $\frac{4Q}{\pi R^3}$ is plotted versus $\frac{1}{R}$ for various shear stress values, so that the value of the slip velocity is equal to the slope of these curves divided by four.

The results of the Mooney analysis for the three polymers under investigation are presented in Figure 6. In all three cases, for the neat polymers the slip velocities are relatively small. For low values of the wall stress, the slip velocities are practically zero, but for high stress values, well into the shear-thinning regime, small but finite slip velocities are obtained, indicating the possibility that the degree of slip at the capillary wall is somehow correlated with the conformation rearrangements and orientation development of the constituent chains imposed by the flow field. However, in all three cases, even at the highest shear rates examined, there appeared to be little slip at the wall.

All three polymers, when combined with additives, displayed significant slip velocities relative to the neat polymers, and this effect became more pronounced with increasing shear stress. For all three of the polymer samples, the ratios of the slip velocities of the neat polymers to polymers plus additive were generally constant, within experimental error, over the entire range of shear stress values. The average values of this ratio taken over all values of shear stress were 0.073 for PP, 0.185 for HDPE, and 0.150 for LDPE. The magnitudes of these ratios provide quantitative comparative measures for the amount of slip enhancement experienced by the particular polymer in the capillary dies, i.e., the smaller this ratio, the greater the degree of viscosity reduction and slip enhancement within the dies.

Flow in Semihyperbolically Converging Dies

Experiments with ACER for the three neat polymers and the polymer plus 2% SA were carried out using four SHCDs with nominal Hencky strain values of 4, 5, 6, and 7. All experiments were conducted at 220°C. Figures 7 and 8 display results for the effect of the SA additive on the apparent elongational viscosity of HDPE and LDPE, with and without additive. (We display only the Hencky values 6 and 7 for LDPE, for conciseness. The data for PP are very similar to that of LDPE, and are also not presented.) For all three polymers, and for all values of Hencky die, the degree of effective stress reduction because of the additive is relatively insensitive to the applied strain rate. Also, the degree of stress reduction is relatively weak, when compared with the shear viscosity data measured in the capillary tubes. The typical range of viscosity reduction is 0–10%. We hypothesize that these observations are because of the enhancement of orientational effects that occur within the SHCDs relative to the capillary dies. Since the SHCDs impose a strong elongational component

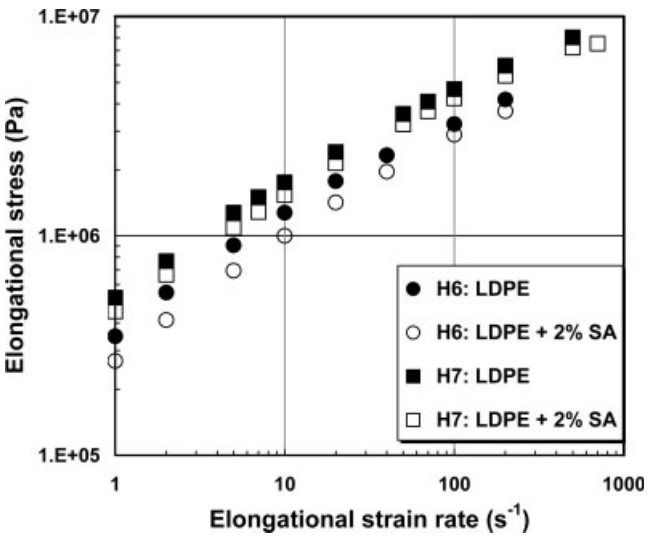

FIG. 8. Effective elongational stress versus strain rate for LDPE and LDPE +2% SA in SHCDs of Hencky values 6 and 7.

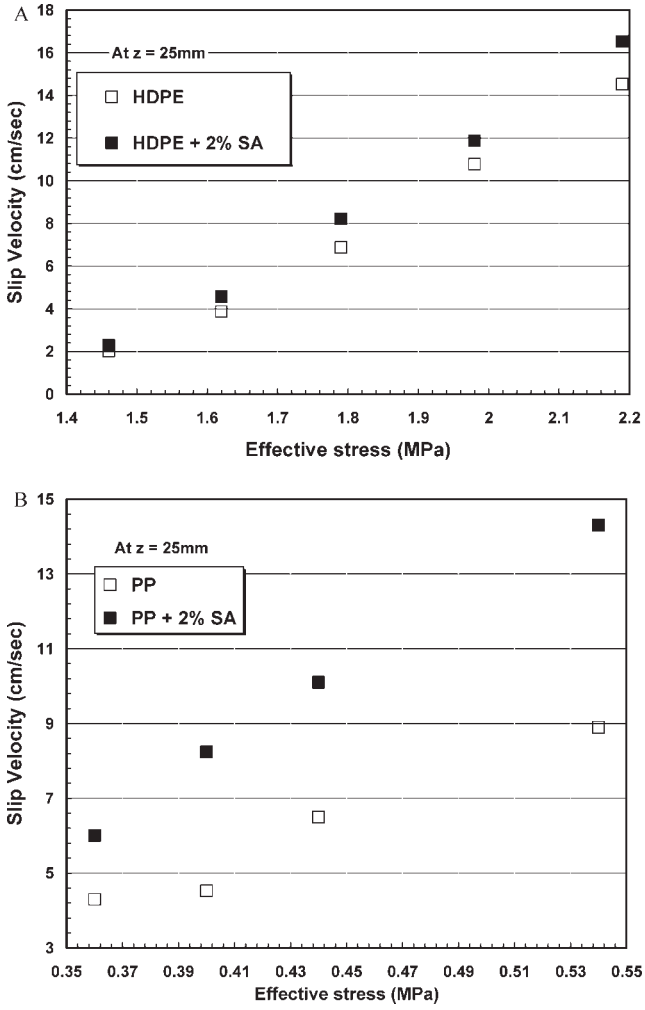

FIG. 9. Slip velocity versus applied stress for (a) HDPE and (b) PP with and without 2% stearic acid additive in SHCDs.

to the flow kinematics, it is very likely that the polymer orientation within these dies is much greater than in the straight-walled capillary tubes. As the samples are highly oriented by the kinematics in the SHCDs even in the absence of the SA, the presence of this additive cannot have as large an impact on the orientational properties of the polymers as it does in purely shear flow.

Note that in all three cases, the degree of stress reduction decreases as the Hencky value of the die increases (although this effect cannot be discerned well from the logarithmic plots presented herein) for all values of strain rates. For the HDPE data presented in Figure 7, the effect of the additive is essentially completely insignificant already for a SHCD of Hencky value 6. For the LDPE data, the viscosity reduction is still evident at Hencky 7, although it has been substantially reduced relative to the other SHCDs of lesser Hencky values. Because of the elongational character of the kinematics in these dies, it is apparent that a high degree of orientation is induced in the polymer samples as they flow through the dies. As the Hencky value of the die increases, the degree of orientation will increase as well. Hence, once again, we observe direct experimental evidence from Figures 7 and 8 that the enhanced orientation of the polymer samples mitigates the effect of the additive, i.e., the additive does not alter the orientational state of the polymer chains to as significant of a degree since the chains are already strongly oriented even in the absence of the additive.

The modified Mooney analysis discussed in Analysis of the Slip Velocity in Semihyperbolically Converging Dies Section was applied to the data presented earlier to calculate an effective slip velocity at the die exit ($z = 25$ mm). Plots of $\left(\frac{Q}{\pi R^3} - \frac{\dot{\varepsilon}_z}{R}\right)$ vs. $\frac{1}{R}$, similar to those of Figure 5, were constructed for various specific values of the measured fluid stress. Again, evaluation of the slopes of the resulting curves allowed calculation of the presumed slip velocity of the fluid at the die exit.

Figure 9 displays plots of slip velocity versus effective stress $\left(\frac{\Delta P}{\dot{\varepsilon}_h}\right)$ for HDPE and PP, with and without the additive. (The plot of LDPE was similar to that of PP, and is not presented for conciseness. It is assumed that the wall shear stress is proportional to the effective stress, but in this approximate analysis, there is no way to determine accurately the exact value of the wall stress.) In all three cases, the slip velocity of the neat polymers was significant on an absolute basis, even at low strain rates, indicating that pronounced slip occurs within these dies even without the additive. This is in contrast to the capillary dies, wherein the neat polymers did not experience much die slip at all. This effect is amplified by the fact that the effective strain rates applied in the SHCDs are two orders of magnitude lower than in the capillary dies-compare the abscissas of Figures 7 and 2. Since, we fully expect a much greater degree of orientation to occur in the SHCDs relative to the straight-walled tubes, this seems to imply a direct relationship between the degree of orientation and the magnitude of the slip velocity.

Figure 9 also indicates that the degree of slip enhancement experienced within these dies because of the presence of the additive is relatively small when compared with that which occurs within the capillaries. Again, the enhancement of the chain mobility because of the additive has a lesser effect once the chains are more fully stretched and oriented. This results in only a relatively modest increase in the slip velocities for the polymers with additive in the SHCDs, as opposed to the case for the straight-walled tubes. Again, the linear scale on the ordinates in Figure 9 hides the fact that the additive seems to have a greater effect at low stress values, although this effect is hard to quantify because of the experimental error at low strain rate values.

By calculating an average value for the ratio of the slip velocities of the neat polymers relative to the slip velocities of the polymers plus additive, one obtains the values 0.871 for HDPE, 0.610 for PP, and 0.638 for LDPE. These values are compared with the similar averages from the capillary dies of 0.185 for HDPE, 0.073 for PP, and 0.150 for LDPE. In all cases, the value of this ratio is

 DOI 10.1002/pen

much greater for the same polymer in the SHCDs than in the straight-walled capillaries, even though the effectively applied strain rate is much lower in the SHCDs. (Recall that the value for this ratio is fairly independent of the stress value in both the capillary and SHCDs.) This again lends credence to the hypothesis that the degree of orientation induced in the flowing polymer is directly related to the degree of slip occurring within the material.

SUMMARY

Experiments were conducted to measure the stress reduction occurring after adding SA to three different polymer samples, in both straight-walled capillary tubes and SHCDs. This stress reduction was much more severe in the capillaries, presumably because the neat polymer experienced a greater degree of slip in the SHCDs relative to the straight-walled tubes. Slip velocities for the samples were calculated from the experimental data, with and without additive. These showed that the increase in slip velocity because of the action of the additive was much less in the SHCDs than in the capillaries. It was hypothesized that the degree of wall slip was related to the orientational state within the fluid, and that the SHCDs produced a greater degree of orientation than the pure shear flow generated in the capillary dies. Furthermore, a very thin boundary layer of shear flow near to the wall could produce a high degree of orientation therein, even for a relatively low flow rate: shear rate is inversely proportional to the channel width, so a thin boundary layer would produce a relatively high shear rate. For example, for a nominal elongational strain rate of 1 s^{-1}, the shear rate in the boundary layer could be several orders of magnitude larger, depending on the exact width of the boundary layer.

ACKNOWLEDGMENTS

We thank Dr. B. Jiang and Dr. D.J. Keffer for lending their expertise to this research in the form of useful advice and constructive criticism.

REFERENCES

1. A.V. Ramamurthy, *J. Rheol.*, **30**, 337 (1986).
2. A.V. Ramamurthy, *Adv. Polym. Technol.*, **6**, 489 (1986).
3. D.S. Kalika and M.M. Denn, *J. Rheol.*, **31**, 815 (1987).
4. F.R. Lim and W.R. Schowalter, *J. Rheol.*, **33**, 1359 (1989).
5. S.G. Hatzikiriakos and J.M. Dealy, *J. Rheol.*, **35**, 497 (1991).
6. S.G. Hatzikiriakos and J.M. Dealy, *J. Rheol.*, **36**, 703 (1992).
7. P.A. Drada and S.Q. Wang, *Phys. Rev. Lett.*, **75**, 2698 (1995).
8. S.G. Hatzikiriakos, *Abst. Amer. Chem. Soc.*, **209**, 12 (1995).
9. S.H. Anastasiadis and S.G. Hatzikiriakos, *J. Rheol.*, **42**, 795 (1998).
10. V. Mhetar and L.A. Archer, *Macromolecules*, **31**, 8607 (1998).
11. Y.L. Yeow, H.L. Lee, A.R. Melvani, and G.C. Mifsud, *J. Rheol.*, **47**, 337 (2003).
12. S. Ahn and J.L. White, *J. Appl. Polym. Sci.*, **90**, 1555 (2003).
13. S.G. Hatzikiriakos, C.W. Stewart, and J.M. Dealy, *Int. Polym. Process.*, **8**, 30 (1993).
14. S.G. Hatzikiriakos, P. Hong, W. Ho, and C.W. Stewart, *J. Appl. Polym. Sci.*, **55**, 595 (1995).
15. J.M. Piau, N. Kissi, and A. Mezghani, *J. Non-Newtonian Fluid Mech.*, **59**, 11 (1995).
16. E.E. Rosenbaum and S.G. Hatzikiriakos, *AIChE J.*, **43**, 598 (1997).
17. J.R. Barone and S.Q. Wang, *J. Non-Newtonian Fluid Mech.*, **91**, 31 (2000).
18. E.C. Achilleos, G. Georgiou, and S.G. Hatzikiriakos, *J. inyl Addit. Technol.*, **8**, 7 (2002).
19. S.G. Hatzikiriakos, *J. Vinyl Addit. Technol.*, **8**, 223 (2002).
20. S. Ahn and J.L. White, *Int. Polym. Process.*, **18**, 243 (2003).
21. S.G. Hatzikiriakos and N. Rathod, *Korea Aust. Rheol. J.*, **15**, 173 (2003).
22. M. Sentmanat and S.G. Hatzikiriakos, *Rheol. Acta*, **43**, 624 (2004).
23. N. Rathod and S.G. Hatzikiriakos, *Polym. Eng. Sci.*, **44**, 1543 (2004).
24. E.B. Muliawan, S.G. Hatzikiriakos, and M. Sentmanat, *Int. Polym. Process.*, **20**, 60 (2005).
25. M. Mooney, *J. Rheol.*, **2**, 210 (1931).
26. J.R. Collier, O. Romanoschi, and S. Petrovan, *J. Appl. Polym. Sci.*, **69**, 2357 (1998).
27. S. Petrovan, J.R. Collier, and G.H. Morton, *J. Appl. Polym. Sci.*, **77**, 1369 (2000).
28. K. Feigl, F.X. Tanner, B.J. Edwards, and J.R. Collier, *J. Non-Newtonian Fluid Mech.*, **115**, 191 (2003).